© 2017. Published by The Company of Biologists Ltd | Journal of Cell Science (2017) 130, 111-118 doi:10.1242/jcs.188169

SPECIAL ISSUE: 3D CELL BIOLOGY

SHORT REPORT

EphA2 proteomics in human keratinocytes reveals a novel association with afadin and epidermal tight junctions

Bethany E. Perez White[1], Rosa Ventrella[1], Nihal Kaplan[1], Calvin J. Cable[1], Paul M. Thomas[2,3] and Spiro Getsios[1,4,*,‡]

ABSTRACT

EphA2 is a receptor tyrosine kinase that helps to maintain epidermal tissue homeostasis. A proximity-dependent biotin identification (BioID) approach was used to identify proteins in close proximity to EphA2 within primary human keratinocytes and three-dimensional (3D) reconstituted human epidermis (RHE) cultures to map a putative protein interaction network for this membrane receptor that exhibits a polarized distribution in stratified epithelia. Although a subset of known EphA2 interactors were identified in the BioID screen, >97% were uniquely detected in keratinocytes with over 50% of these vicinal proteins only present in 3D human epidermal culture. Afadin (AFDN), a cytoskeletal and junction-associated protein, was present in 2D and 3D keratinocyte cultures, and validated as a so-far-unknown EphA2-interacting protein. Loss of EphA2 protein disrupted the subcellular distribution of afadin and occludin in differentiated keratinocytes, leading to impairment of tight junctions. Collectively, these studies illustrate the use of the BioID approach in order to map receptor interaction networks in 3D human epithelial cultures, and reveal a positive regulatory role for EphA2 in the organization of afadin and epidermal tight junctions.

KEY WORDS: Afadin, Keratinocytes, Proteomics, 3D culture, EphA2, Tight junction

INTRODUCTION

Receptor tyrosine kinases (RTKs) are key regulators of epithelial tissue homeostasis and are molecular targets in several diseases (Schlessinger, 2014). Yet, our knowledge of RTK signaling largely comes from work in two-dimensional (2D) cultures frequently employing transformed cell lines or mouse models. Although these experimental approaches have advanced our understanding of RTK action, they do not fully take into account the architectural complexity of human tissues, particularly for stratified epithelia, such as the epidermis where RTKs are positioned in specific cell layers and membrane locations.

To address this knowledge gap, we focused on mapping the putative interactome of a prototypical RTK, EphA2. EphA2 interacts with ephrins on adjacent cells to regulate epithelial tissue homeostasis (Perez White and Getsios, 2014). Specifically, loss of EphA2 increased susceptibility to chemically-induced skin carcinogenesis (Guo et al., 2006), whereas ephrin-targeting of EphA2 enhanced keratinocyte adhesion and differentiation (Lin et al., 2010; Walsh and Blumenberg, 2011). EphA2 can positively or negatively regulate intercellular junctions, including tight junctions (Zhou et al., 2011; Tanaka et al., 2005; Larson et al., 2008; Miao et al., 2014; Miura et al., 2009) that contribute to skin barrier function (Niessen, 2007). Importantly, EphA2 is expressed in a differentiation-dependent, polarized manner within human epidermis (Fig. 1A).

We adapted the method of unbiased, proximity-dependent biotin identification (BioID) (Roux et al., 2012) to identify near neighbors of EphA2 in normal human epidermal keratinocytes (NHEKs) grown as 2D sheets undergoing Ca^{2+}-dependent differentiation during which EphA2 is recruited to cell-cell borders (Lin et al., 2010), or three-dimensional (3D) reconstituted human epidermis (RHE), in which EphA2 is concentrated at suprabasal cell–cell contacts (Gordon et al., 2013). We compared the EphA2 interactome in 2D and 3D cultures obtained by using BioID, and assessed the impact of EphA2 loss on the distribution of afadin and on epidermal tight junctions.

RESULTS AND DISCUSSION

Characterization of EphA2 biotin ligase fusion protein in 2D and 3D keratinocyte cultures

To characterize the EphA2 interactome in human keratinocytes, we utilized BioID (Roux et al., 2012) and fused a hemagglutinin (HA)-tagged bacterial biotin ligase (BirA*) to the C-terminus of EphA2 (this fusion protein is hereafter referred to as EphA2*) which was transduced into NHEKs. In 2D cultures maintained in high [Ca^{2+}] (1.2 mM), EphA2* was immunolocalized to cell borders together with endogenous EphA2 and biotinylated proteins as detected by streptavidin reactivity after 24 h in medium supplemented with biotin (50 µM, Fig. 1B); this accumulation of biotinylated proteins was time-dependent (Fig. 1C). Similarly, most biotinylated proteins detected in 3D RHE localized to the cell periphery (Fig. 1D), mirroring the distribution of endogenous EphA2 in human epidermis (Fig. 1A). EphA2* did not interfere with normal differentiation as assessed by analyzing the level of desmoglein 1 (Getsios et al., 2004) (Fig. 1E). These findings suggest that BioID can be used to detect membrane-proximal EphA2-interacting proteins that impact keratinocyte signaling.

BioID revealed proteins that putatively interact with EphA2 in keratinocytes

Our overarching goal was to generate a list of potential EphA2 interactors associated with keratinocyte differentiation. For 2D cultures, confluent NHEKs were maintained in high [Ca^{2+}] for 1 h or 24 h, conditions under which EphA2 is concentrated at cell–cell borders (Lin et al., 2010); then biotin was added for another 24 h. In

[1]Department of Dermatology, Northwestern University, Chicago, IL 60611, USA. [2]Proteomics Center of Excellence, Northwestern University, Chicago, IL 60611, USA. [3]Department of Molecular Biosciences, Northwestern University, Chicago, IL 60611, USA. [4]Cell and Molecular Biology, Northwestern University, Chicago, IL 60611, USA.
*Present address: GlaxoSmithKline, UP1410, 1250 South Collegeville Rd., Collegeville, PA 19426, USA.

‡Author for correspondence (spigetsi@gmail.com)

S.G., 0000-0002-1141-4562

Received 16 February 2016; Accepted 31 October 2016

Journal of Cell Science (2017) 130, 111-118 doi:10.1242/jcs.188169

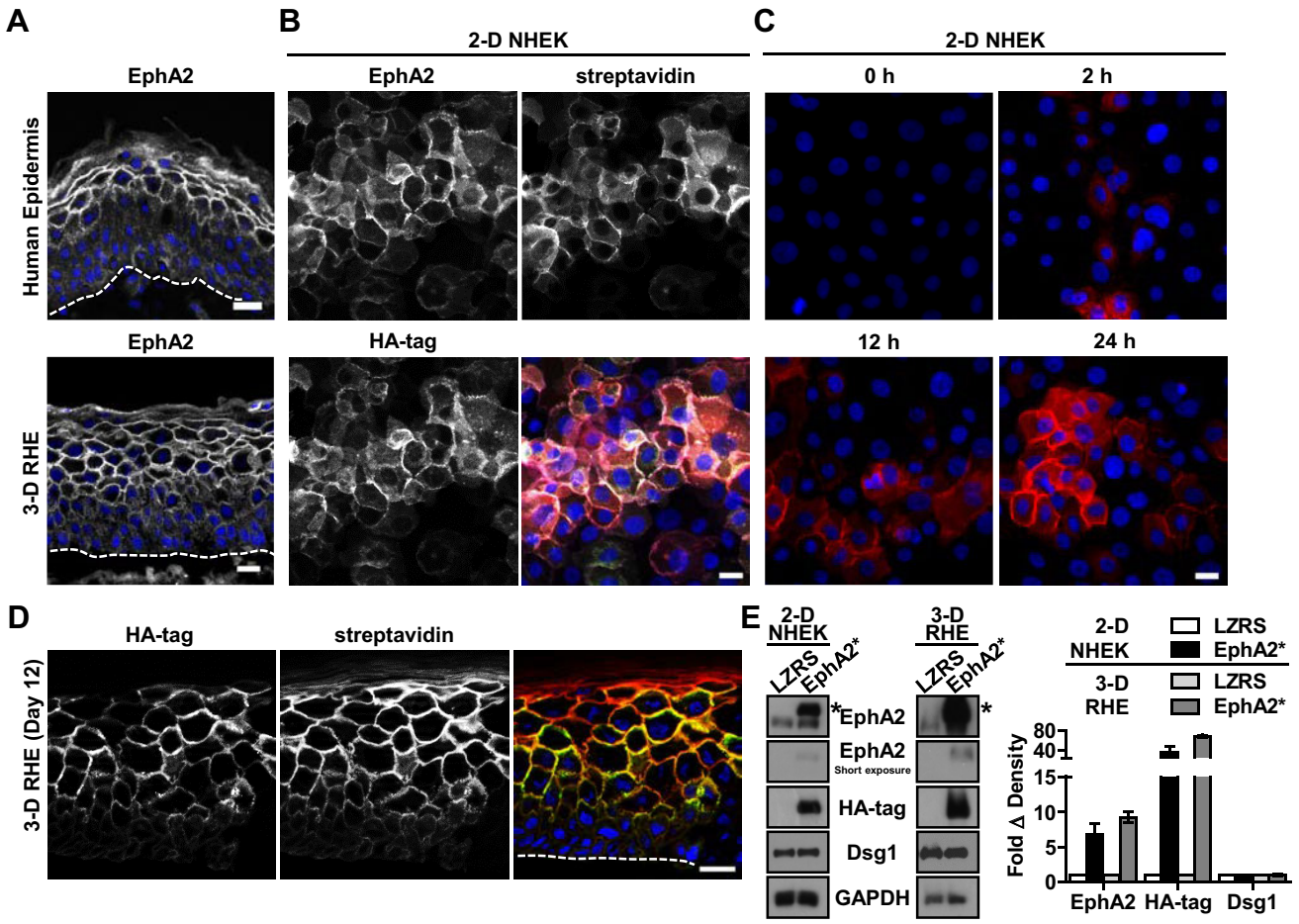

Fig. 1. EphA2* characterization in 2D and 3D cultures. (A) Endogenous EphA2 localization in human epidermis and 3D RHE. (B) Localization of EphA2* (EphA2 and HA-tag) and distribution of biotinylated proteins as shown by streptavidin reactivity following 24 h exposure to biotin in high [Ca^{2+}]. (C) Time course of protein biotinylation in EphA2*-expressing NHEKs. (D) Localization of EphA2* (HA-tag) and biotinylated proteins in 3D RHE. (E) Analysis and quantification of proteins in 2D and 3D cultures in empty vector (LZRS) or EphA2*. Dsg1, desmoglein 1 (n=3; mean±s.e.m.). *, HA-tagged EphA2*. The dashed lines indicate basement membrane. Scale bars: 20 µm.

3D RHE, tissues were harvested at days 3, 6, 9 and 12 following 72 h of treatment with biotin. Samples of differentiated keratinocytes were collected in an 8 M urea buffer to comprehensively solubilize their cellular components. The peptide spectral matches (PSMs) of proteins from all time points in 2D or 3D culture samples from three independent mass spectrometry experiments were combined, respectively, for downstream bioinformatics to gather a broad spectrum of EphA2-interacting proteins during keratinocyte differentiation. Inclusion criteria and the full list of putative EphA2 interactors in 2D and 3D cultures are available in supplementary File 1.

In the 2D and 3D BioID screens, 131 and 215 proteins, respectively, were identified. Proteins were classified by gene ontology according to protein class by using the Protein ANalysis THrough Evolutionary Relationships (PANTHER) database (Mi et al., 2016). The top three protein classes identified by using the PANTHER analysis were common in 2D and 3D cultures, and included cytoskeletal proteins, membrane trafficking proteins and enzyme modulators (Fig. 2A). However, the relative abundance of candidate proteins in these and less-represented gene ontology categories revealed key differences, with increased levels of cell junction and cell adhesion molecules in 2D cultures, and more prominent coverage of enzyme modulators, hydrolases, and Ca^{2+}-binding proteins in 3D RHE. Analysis by using the Kyoto Encyclopedia of Genes and Genomes (KEGG) database (Kanehisa and Goto, 2000) illustrated additional biological pathways shared between 2D and 3D cultures, particularly with respect to endocytosis, tight junctions and Rap1 signaling (Fig. 2B). Interestingly, focal adhesion proteins were prominent in 2D cultures, whereas cancer-related and metabolic pathways were evident in 3D RHE.

The top 50 protein hits from 2D and 3D cultures (Fig. 2C) were subjected to Pearson's correlation coefficient statistical analysis, revealing significant concordance (R^2=0.6651, P<0.0001, Fig. 2D). Of the proteins identified in 2D and 3D culture, 76 overlapped (2D: 58%; 3D: 35%, Fig. 2E). Notably, only six of the 74 proteins previously shown to interact with EphA2 – as obtained from the BioGRID (Chatr-Aryamontri et al., 2015) and IntAct (Orchard et al., 2014) databases – were found in the BioID-defined EphA2 interactome. This possibly reflects cell-type-specific differences or the result of fusing BirA* to the extreme cytoplasmic terminus of EphA2. Accordingly, SHIP2 (officially known as INPPL1) is a well-characterized cytoplasmic binding partner of EphA2 (Lee et al., 2012) that was detected in the EphA2* interactome of 2D (#73) and 3D cultures (#141); this EphA2–SHIP2 interaction was further confirmed in NHEKs in co-immunoprecipitation (co-IP, Fig. S1) assays. In contrast, the Eph receptor ligand ephrin-A1 (EFNA1), which interacts with the extracellular domain of EphA2, was not present in the EphA2 interactome. Interestingly, our BioID

Journal of Cell Science (2017) 130, 111-118 doi:10.1242/jcs.188169

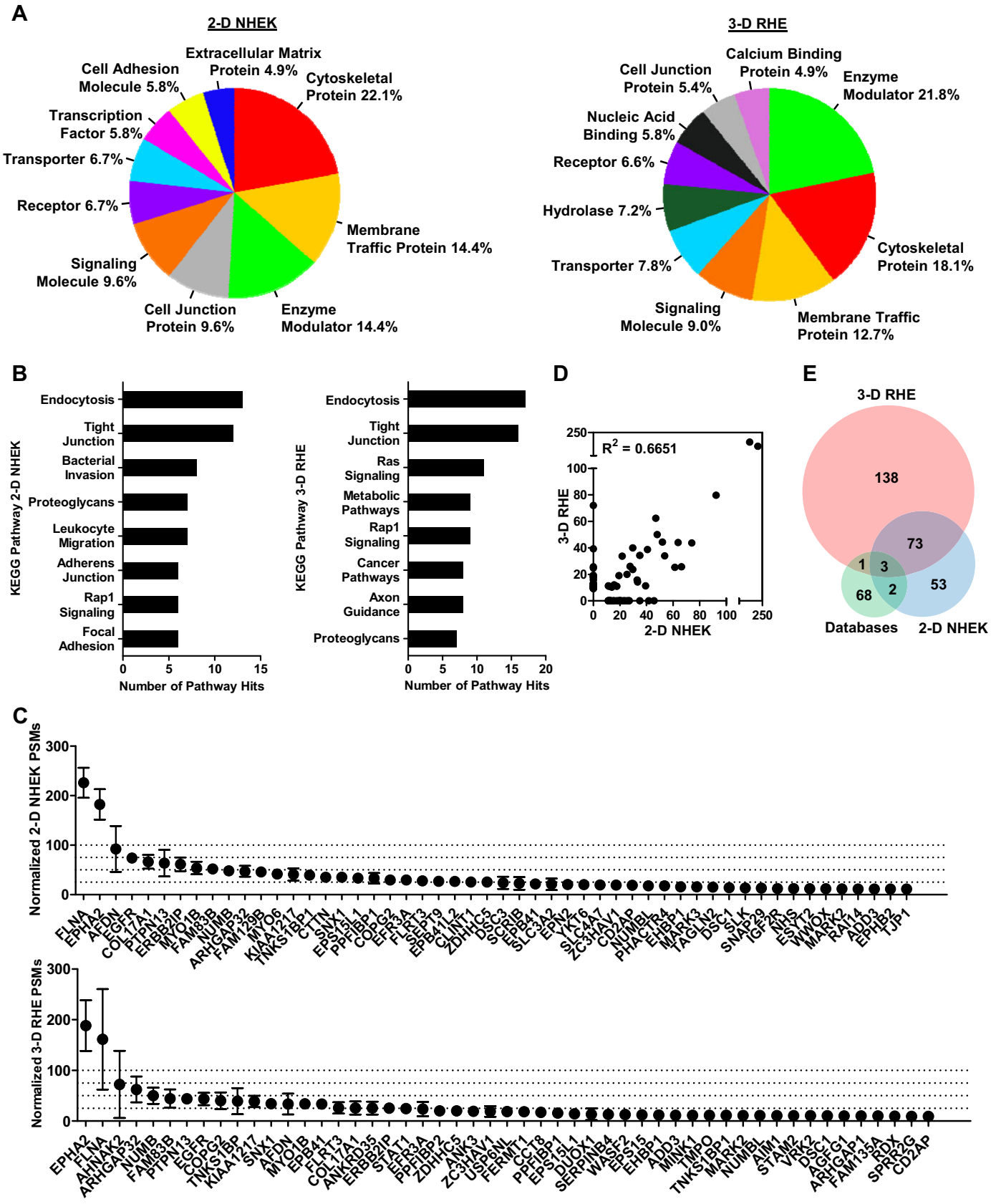

Fig. 2. Proteomic analysis of putative EphA2-interacting proteins in NHEKs. (A,B) PANTHER database gene ontology classification of protein class (A) and KEGG pathway analysis of EphA2-interacting proteins in 2D NHEK and 3D RHE cultures (B). (C) Top 50 hits in 2D and 3D cultures ranked by PSMs. (n=3; mean± s.e.m.). (D) Pearson's correlation of the PSMs from the top 50 hits in 2D and 3D cultures (P<0.0001). (E) Overlap of BioID-characterized proteins between 2D NHEK culture, 3D RHE and annotated EphA2 interactors in the BioGRID and IntAct databases.

Journal of Cell Science (2017) 130, 111-118 doi:10.1242/jcs.188169

analysis of primary keratinocytes did not identify E-cadherin, which was shown to be an EphA2 interactor in other epithelial cells (Van Itallie et al., 2014; Guo et al., 2014; Zantek et al., 1999). Taken together, the BioID analysis of the EphA2 interactome derived from primary human keratinocytes has greatly expanded the catalogue of putative proteins that may operate in concert with this RTK to regulate epithelial tissue homeostasis.

EphA2 and afadin interact in keratinocytes

Afadin is an actin-binding protein associated with nectin and cadherin-based adherens junctions, as well as tight junctions (Yamamoto et al., 1997; Ooshio et al., 2010; Mandai et al., 1997; Indra et al., 2014; Choi et al., 2016; Monteiro et al., 2013). Afadin was a high-ranking hit in our EphA2 BioID screen (2D, #3; 3D, #13). In addition to its role as a cytoskeleton–junction linker, afadin has been implicated in tight junction regulation (Yamamoto et al., 1997; Ooshio et al., 2010; Monteiro et al., 2013; Choi et al., 2016; Mandai et al., 1997). We found that loss of afadin in NHEKs disrupted organization and function of tight junctions (Fig. S2). Other Eph family members have been linked to afadin in fibroblast cell lines following its exogenous overexpression (Hock et al., 1998) but a native complex with EphA2 has not been described. As EphA2 is involved in contact-dependent signaling events and our BioID screen revealed a strong association with cytoskeletal proteins, cell junctions and tight-junction biology that, collectively, have been linked to afadin function, we examined this putative interaction in more detail.

BioID can detect proximal proteins that do not necessarily interact with the protein of interest, so we examined endogenous EphA2–afadin complexes in keratinocytes. Afadin co-immunoprecipitated with EphA2 in 2D cultures (Fig. 3A). Proximity ligation assays (PLAs) also indicated EphA2 and afadin interact in NHEKs (Fig. 3B). Although EphA2–afadin puncta were present throughout NHEKs – suggesting multiple sites of close association – EphA2 and afadin were prominently localized at cell borders as visualized following conventional immunostaining (Fig. 3C). In 3D RHE afadin had a relatively diffuse distribution pattern within its lower layers. This was similar to afadin distribution in human epidermis in which EphA2 and afadin overlap was limited (Fig. S3), but in which partial colocalization was also evident at cell–cell contacts within the uppermost epidermal layers that do have tight junctions (Fig. 3C). Colocalization analysis showed a significant overlap of EphA2 and afadin in 2D NHEKs, 3D RHE and human epidermis (Fig. 3D). These results authenticate afadin as a bona fide EphA2-interacting protein in human keratinocytes and indicate that these two proteins can cooperate in the suprabasal layers of the epidermis to regulate tight junctions.

EphA2-deficient keratinocytes have tight junction defects

In view of EphA2 and afadin colocalization in the uppermost layers of the epidermis, we asked whether loss of EphA2 impacts tight junctions. Previous studies have shown that EphA2 interacts with occludin and claudin-4 (Fredriksson et al., 2015; Tanaka et al., 2005). Our EphA2 BioID screen also yielded occludin as a low-abundance hit (2D, #131; 3D, #102), whereas claudin-4 was undetectable. Instead, other tight junction proteins were found in 2D (claudin-1, #120; zonula occludens 1 and 2, #52; #115, respectively) and 3D (claudin-1, #158, junctional adhesion molecule A, #186) cultures. As afadin was a major hit in both 2D and 3D cultures, and is linked to tight junctions, we focused on the consequence loss of EphA2 has on afadin localization and tight junction function.

Loss of EphA2 altered afadin localization in 2D cultures from a predominantly junctional to more cytoplasmic distribution (Fig. 3C). Coinciding with defects in the morphogenesis of suprabasal epidermis in 3D RHE that lacked EphA2, afadin was no longer concentrated at junctions in the uppermost stratified layers (Fig. 4A) where it usually overlaps with occludin (Fig. 4B). These results indicate that EphA2 helps to maintain the junctional distribution of afadin in the suprabasal epidermis.

Since occludin is restricted to the junctions of the upper granular layer of the epidermis (Morita et al., 1998) where there is a higher concentration of EphA2 and afadin, we examined occludin distribution as an indicator of tight junction organization. In whole-mount preparations of 3D RHE, loss of EphA2 delayed the junctional distribution of occludin in suprabasal epidermis at day 6 and grossly disrupted the tight junction network after 12 days (Fig. 4C). Likewise, there was perturbation of the occludin junctional network in EphA2-deficient NHEKs exposed to high [Ca^{2+}] over 7 days in 2D culture (Fig. 4D). Despite the delay in occludin junctional localization at earlier time points in EphA2-deficient keratinocytes, a significant decrease in trans-epithelial electrical resistance (TEER) was not apparent until day 7 compared to empty vector-transduced control cells. (Fig. 4E). We further assayed the integrity of the tight junction barrier by Ca^{2+} withdrawal and restoration. (Van Itallie et al., 2014). After overnight withdrawal, medium was replenished with Ca^{2+} for 24 h. Control NHEKs but not EphA2-deficient cells were able to recover, as evidenced by increased TEER (Fig. 4E). We also tested for paracellular permeability by using a fluorescein isothiocyanate (FITC)–dextran flux assay. Similar to TEER, there was a significant impairment of barrier function at day 7 and following Ca^{2+} recovery (Fig. 4F). We further assessed the impact of EphA2 loss on tight junction function in A431 epidermoid carcinoma cells (Fig. S4). EphA2-deficiency significantly impaired the localization of afadin and occludin, and the Ca^{2+}-dependent reformation of tight junctions in A431 cells, providing additional support for its role in tight junction organization and function. Our findings differ from previous studies that have indicated that EphA2 negatively regulates tight junctions (Larson et al., 2008; Miao et al., 2014; Zhou et al., 2011), including through direct phosphorylation of claudin-4 (Tanaka et al., 2005). However, our data are more in line with the ability of EphA2 to promote differentiation-associated junctions in polarized epithelial cells and keratinocytes (Lin et al., 2010; Walsh and Blumenberg, 2011; Miura et al., 2009), and provide additional support for the concept that differentiation state and tight junctions are closely linked within epidermal keratinocytes in a manner that depends on EphA2.

Although further studies must be performed to delineate the precise role of EphA2 in epidermal tight junctions and the extent to which this relies on interaction with afadin, our BioID results provide insight into possible mechanisms. For example, Rap1 signaling molecules – which are known afadin modulators – were identified by KEGG analysis in the putative EphA2 interactome. Afadin translocation was decreased in endothelial cells that lack Rap1 (Birukova et al., 2012) and afadin–Rap1 signaling propagated endothelial barrier recovery through Rho inhibition (Birukova et al., 2013). Afadin has been shown to function downstream of Rap1 signaling (Kooistra et al., 2007) or as its upstream co-activator (Severson et al., 2009). It is interesting to speculate whether EphA2 plays a role as an upstream activator of the Rap1 pathway leading to afadin and tight junction stabilization.

In conclusion, we have used BioID to define potential EphA2-binding partners in 2D NHEK and 3D RHE cultures, which has greatly expanded the putative EphA2 interactome, and uncovered a link between afadin and tight junction organization. The adaptation of BioID for 3D human epidermal cultures, therefore, permits

Journal of Cell Science

Journal of Cell Science (2017) 130, 111-118 doi:10.1242/jcs.188169

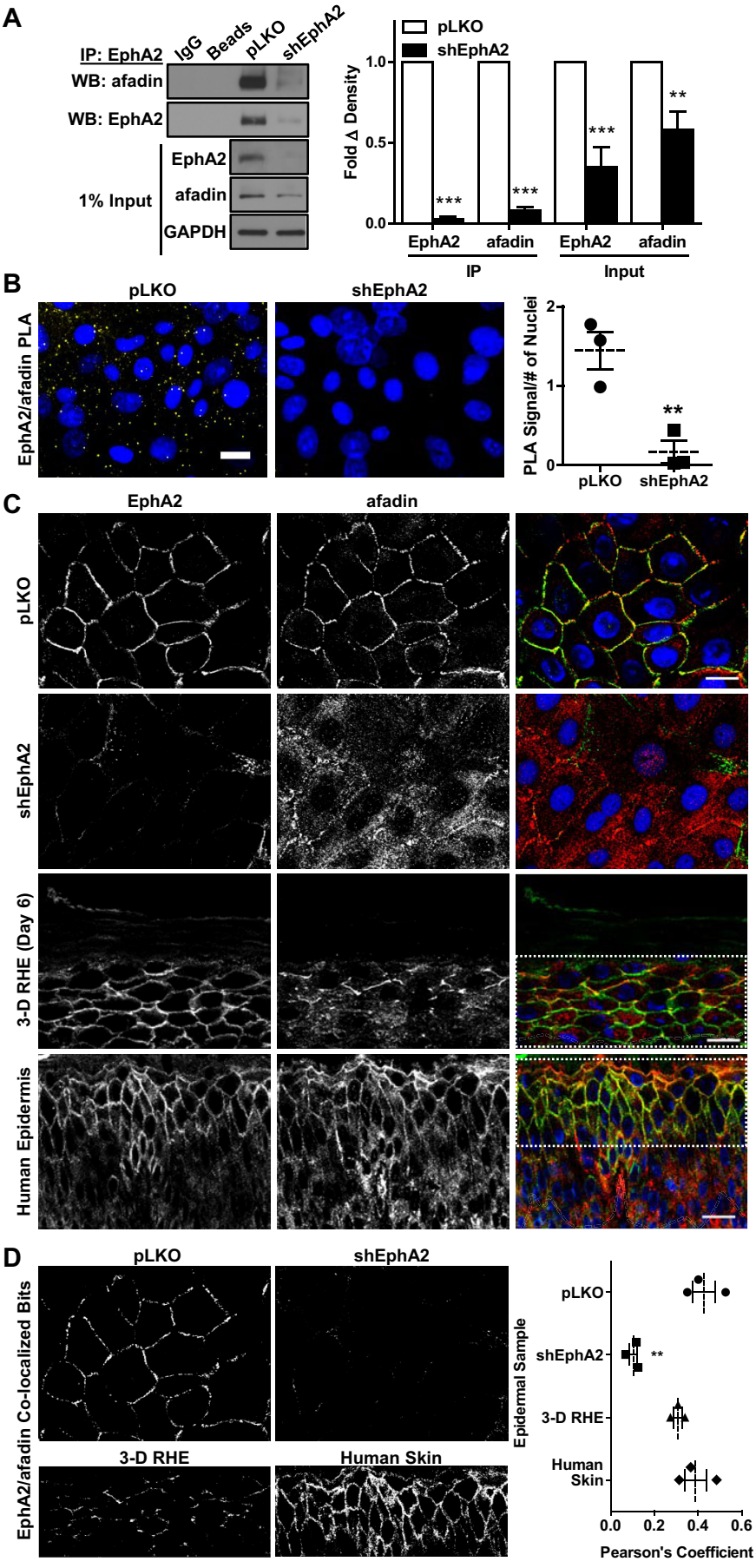

Fig. 3. Validation of interaction between EphA2 and afadin. (A) Co-IP analysis of EphA2 and afadin (n=3; mean±s.e.m.) $^{**}P$<0.01; $^{***}P$<0.001 (two-way ANOVA and Bonferroni post-test). (B) PLA analysis of EphA2 and afadin (n=3; mean±s.e.m.) $^{**}P$=0.0019 (one-tailed t-test). (C) Localization of EphA2 and afadin in 2D and 3D cultures and human epidermis. (D) Quantification of colocalized EphA2 and afadin from colocalized bits. For analysis in 3D RHE and epidermis, regions in the upper epidermal layers were analyzed (boxed area). (n=3; mean±s.e.m.) $^{**}P$=0.0016 (one-way ANOVA). Scale bars: 20 µm; pLKO, empty vector control; shEphA2, lentiviral knockdown of EphA2.

Journal of Cell Science (2017) 130, 111-118 doi:10.1242/jcs.188169

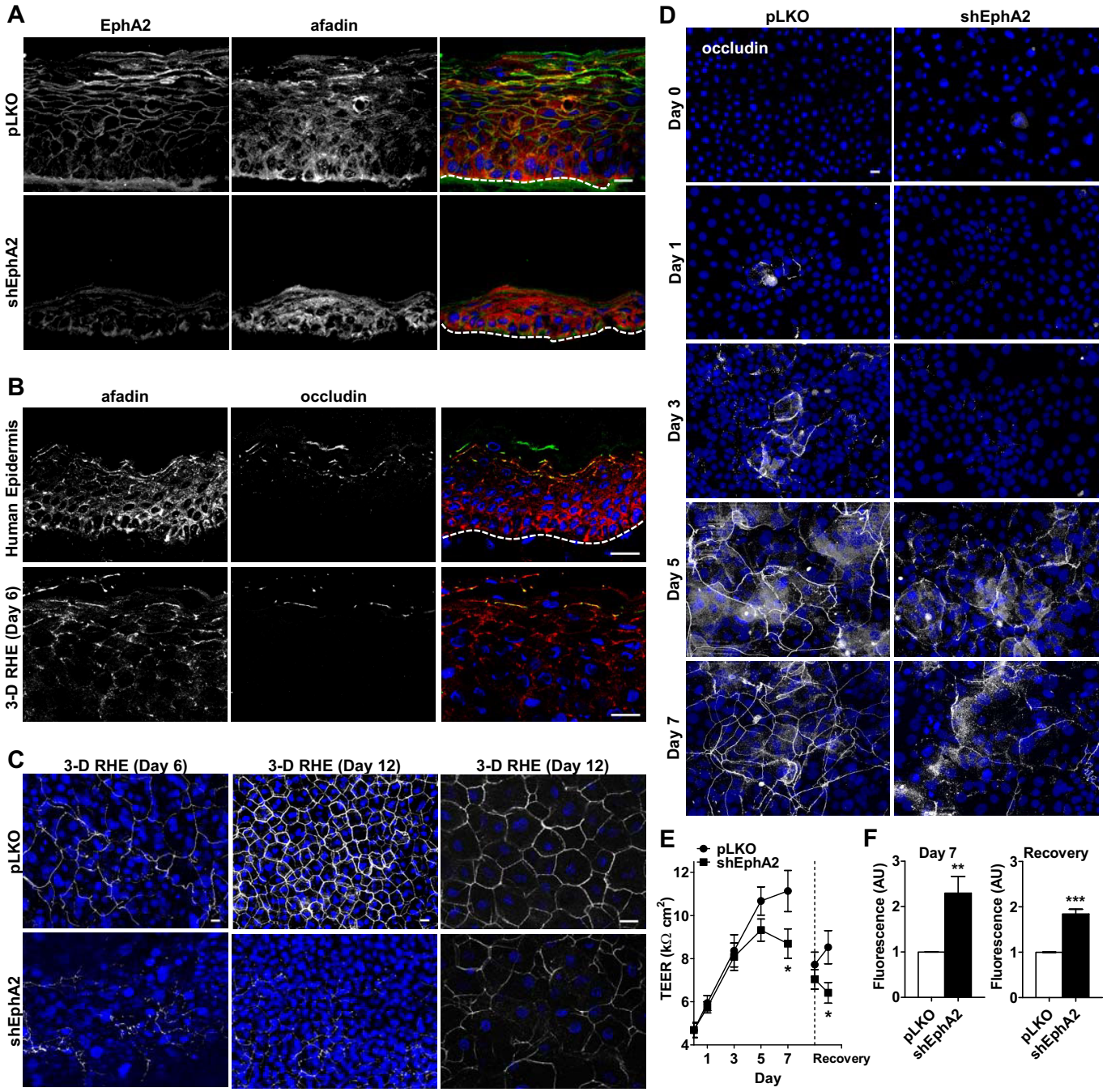

Fig. 4. Loss of EphA2 disrupts epidermal tight junctions. (A) Immunofluorescence of afadin in pLKO control versus shEphA2 in 3D RHE. (B) Localization of afadin and occludin in human epidermis and 3D RHE. (C) Occludin immunostaining in whole-mount preparations of pLKO and shEphA2 3D RHE in en face view. (D) Time course of occludin expression in 2D pLKO and shEphA2 cultures. (E) Quantification of TEER assay in 2D cultures. The dotted vertical line represents TEER after Ca^{2+} withdrawal and recovery. Recovery represents TEER 24 h after replacing Ca^{2+} (n=11; mean±s.e.m.) *P<0.05 (one-tailed Student's t-test). (F) FITC–dextran flux in pLKO and shEphA2 2D NHEK cultures (n=3; mean±s.e.m.) **P=0.0063; ***P=0.0006 (one-tailed t-test). The dashed lines indicate the basement membrane; scale bars: 20 µm.

identification of potentially physiologically relevant interaction networks of proteins that exhibit a polarized distribution in stratified epithelia, including EphA2.

MATERIALS AND METHODS

Cell culture

Normal human epidermal keratinocytes (NHEKs) were isolated from neonatal foreskins and cultured as described (Simpson et al., 2010). Cells of the human epidermoid carcinoma cell line (A431) were obtained from American Type Culture Collection (ATCC; Manassas, VA) and cultured as specified without authentication.

Cloning and viral production

pcDNA3.1-MCS-BirA(R118G)-HA was a gift from Kyle Roux (plasmid #36047, Addgene, Cambridge, MA) (Roux et al., 2012). BirA* was PCR-fused to EphA2 (EphA2*), digested into the LZRS backbone and packaged in Phoenix retroviral packaging cells (ATCC) (Getsios et al., 2004). The pLKO constructs were gifts from Bingcheng Wang (Case Western Reserve University, Cleveland, OH) and were packaged in HEK293T (ATCC) cells.

Antibodies
Antibody information is available in Table S1.

Immunofluorescence
Immunofluorescence was performed using conventional protocols. Whole-mount preparations were performed as described, with an initial fixation in 1% formalin (Pal-Ghosh et al., 2008). Images were captured by using a Zeiss AxioImager Z.1 microscope with ApoTome (Carl Zeiss AG, Oberkochen, Germany). FIJI software (http://fiji.sc/) was used to quantify colocalization and determine Pearson's coefficients (Schindelin et al., 2012). For analysis in 3D RHE and human epidermis, a 1376×601 pixel region of interest taken from the upper layers was quantified. For each replicate, six fields were analyzed.

Proteomics
BioID was performed according to Roux et al. (2013). For BioID in 2D NHEK and 3D RHE, cultures were incubated with biotin for 24 h and 72 h, respectively, prior to harvest. Following on-bead trypsinization, peptides were desalted and eluted into 80% acetonitrile/0.2% formic acid, lyophilized, reconstituted with 0.2% formic acid, and injected onto a trap column-coupled nanobore column. Peptides were then separated by using a linear gradient of 95% water, 5% acetonitrile, 0.1% formic acid and 5% water, 95% acetonitrile, 0.1% formic acid. Mass spectrometry data were obtained on a Velos Orbitrap Elite (Thermo Fisher Scientific, Grand Island, NY) and searched using Mascot 2.5 (Matrix Science, Boston, MA) against the SwissProt database (Boutet et al., 2007). Results were reported at 1% false discovery rate in Scaffold 4 (Searle, 2010).

Western blotting and co-immunoprecipitation assays
Western blotting and co-IPs were performed by using standard procedures.

Proximity ligation assay
The Duolink kit (Sigma-Aldrich, St Louis, MO) was used and the signal was analyzed with Image J (Schneider et al., 2012). For each replicate, ten fields were analyzed.

Barrier assays
Trans-epithelial electrical resistance (TEER) was measured by using an epithelial Volt/Ohm meter (EVOM; World Precision Instruments, Inc., Sarasota, FL). Paracellular permeability was assessed using 1 µg FITC–dextran incubated for 30 min (10,000 MW; Sigma). Fluorescence was measured with a SpectraMAX GeminiEM plate-reader (Molecular Devices, Sunnyvale, CA). Both assays were performed in transwell plates (0.4 µm pore size; Corning, Inc., Kennebunk, ME). For Ca^{2+} withdrawal, high-Ca^{2+} medium (1.2 mM) was replaced with medium containing 0.03 mM Ca^{2+} overnight; then medium of these cultures was replenished with 1.2 mM Ca^{2+} for 24 h to allow for recovery of the tight junction barrier.

Statistical analysis
Statistics were performed with GraphPad Prism 6.0 (La Jolla, CA); one-way or two-way ANOVA followed by Bonferroni's post-test or *t*-tests were applied as appropriate.

Competing interests
The authors declare no competing or financial interests.

Author contributions
S.G. and B.E.P.W. conceptualized the project, planned experiments, and wrote the paper with input from all authors. B.E.P.W., R.V., N.K. and C.J.C. performed experiments and analyzed data. P.M.T. developed mass spectrometry methodology.

Funding
This work was supported by the National Institutes of Health (NIH) [grant number R01-AR062110 to S.G.], a Skin Disease Research Center Grant [NIH grant number P30-AR057216-01], and NIH training fellowships to B.E.P.W. [grant number T32-AR060710] and R.V. [grant number T32-GM08061]. B.E.P.W. also received support from the Chicago Biomedical Consortium. C.J.C. was supported by the Northwestern Undergraduate Research Program. Proteomics were performed by the Northwestern Proteomics Core Facility [NIH grant numbers P30-CA060553 and P41-GM108569]. Deposited in PMC for release after 12 months.

Supplementary information
Supplementary information available online at
http://jcs.biologists.org/lookup/doi/10.1242/jcs.188169.supplemental

References
Birukova, A. A., Fu, P., Wu, T., Dubrovskyi, O., Sarich, N., Poroyko, V. and Birukov, K. G. (2012). Afadin controls p120-catenin-ZO-1 interactions leading to endothelial barrier enhancement by oxidized phospholipids. *J. Cell. Physiol.* **227**, 1883-1890.

Birukova, A. A., Tian, X., Tian, Y., Higginbotham, K. and Birukov, K. G. (2013). Rap-afadin axis in control of Rho signaling and endothelial barrier recovery. *Mol. Biol. Cell* **24**, 2678-2688.

Boutet, E., Lieberherr, D., Tognolli, M., Schneider, M. and Bairoch, A. (2007). UniProtKB/Swiss-Prot. *Methods Mol. Biol.* **406**, 89-112.

Chatr-Aryamontri, A., Breitkreutz, B.-J., Oughtred, R., Boucher, L., Heinicke, S., Chen, D., Stark, C., Breitkreutz, A., Kolas, N., O'donnell, L. et al. (2015). The BioGRID interaction database: 2015 update. *Nucleic Acids Res.* **43**, D470-D478.

Choi, W., Acharya, B. R., Peyret, G., Fardin, M.-A., Mège, R.-M., Ladoux, B., Yap, A. S., Fanning, A. S. and Peifer, M. (2016). Remodeling the zonula adherens in response to tension and the role of afadin in this response. *J. Cell Biol.* **213**, 243-260.

Fredriksson, K., Van Itallie, C. M., Aponte, A., Gucek, M., Tietgens, A. J. and Anderson, J. M. (2015). Proteomic analysis of proteins surrounding occludin and claudin-4 reveals their proximity to signaling and trafficking networks. *PLoS ONE* **10**, e0117074.

Getsios, S., Amargo, E. V., Dusek, R. L., Ishii, K., Sheu, L., Godsel, L. M. and Green, K. J. (2004). Coordinated expression of desmoglein 1 and desmocollin 1 regulates intercellular adhesion. *Differentiation* **72**, 419-433.

Gordon, K., Kochkodan, J. J., Blatt, H., Lin, S. Y., Kaplan, N., Johnston, A., Swindell, W. R., Hoover, P., Schlosser, B. J., Elder, J. T. et al. (2013). Alteration of the EphA2/Ephrin-A signaling axis in psoriatic epidermis. *J. Invest. Dermatol.* **133**, 712-722.

Guo, H., Miao, H., Gerber, L., Singh, J., Denning, M. F., Gilliam, A. C. and Wang, B. (2006). Disruption of EphA2 receptor tyrosine kinase leads to increased susceptibility to carcinogenesis in mouse skin. *Cancer Res.* **66**, 7050-7058.

Guo, Z., Neilson, L. J., Zhong, H., Murray, P. S., Zanivan, S. and Zaidel-Bar, R. (2014). E-cadherin interactome complexity and robustness resolved by quantitative proteomics. *Sci. Signal.* **7**, rs7.

Hock, B., Bohme, B., Karn, T., Yamamoto, T., Kaibuchi, K., Holtrich, U., Holland, S., Pawson, T., Rubsamen-Waigmann, H. and Strebhardt, K. (1998). PDZ-domain-mediated interaction of the Eph-related receptor tyrosine kinase EphB3 and the ras-binding protein AF6 depends on the kinase activity of the receptor. *Proc. Natl. Acad. Sci. USA* **95**, 9779-9784.

Indra, I., Troyanovsky, R. and Troyanovsky, S. M. (2014). Afadin controls cadherin cluster stability using clathrin-independent mechanism. *Tissue Barriers* **3**, e28687.

Kanehisa, M. and Goto, S. (2000). KEGG: kyoto encyclopedia of genes and genomes. *Nucleic Acids Res.* **28**, 27-30.

Kooistra, M. R. H., Dube, N. and Bos, J. L. (2007). Rap1: a key regulator in cell-cell junction formation. *J. Cell Sci.* **120**, 17-22.

Larson, J., Schomberg, S., Schroeder, W. and Carpenter, T. C. (2008). Endothelial EphA receptor stimulation increases lung vascular permeability. *Am. J. Physiol. Lung Cell. Mol. Physiol.* **295**, L431-L439.

Lee, H. J., Hota, P. K., Chugha, P., Guo, H., Miao, H., Zhang, L., Kim, S.-J., Stetzik, L., Wang, B.-C. and Buck, M. (2012). NMR structure of a heterodimeric SAM:SAM complex: characterization and manipulation of EphA2 binding reveal new cellular functions of SHIP2. *Structure* **20**, 41-55.

Lin, S., Gordon, K., Kaplan, N. and Getsios, S. (2010). Ligand targeting of EphA2 enhances keratinocyte adhesion and differentiation via desmoglein 1. *Mol. Biol. Cell* **21**, 3902-3914.

Mandai, K., Nakanishi, H., Satoh, A., Obaishi, H., Wada, M., Nishioka, H., Itoh, M., Mizoguchi, A., Aoki, T., Fujimoto, T. et al. (1997). Afadin: a novel actin filament–binding protein with one PDZ domain localized at cadherin-based cell-to-cell adherens junction. *J. Cell Biol.* **139**, 517-528.

Mi, H., Poudel, S., Muruganujan, A., Casagrande, J. T. and Thomas, P. D. (2016). PANTHER version 10: expanded protein families and functions, and analysis tools. *Nucleic Acids Res.* **44**, 17.

Miao, Z., Dong, Y., Fang, W., Shang, D., Liu, D., Zhang, K., Li, B. and Chen, Y.-H. (2014). VEGF increases paracellular permeability in brain endothelial cells via upregulation of EphA2. *Anat. Rec.* **297**, 964-972.

Miura, K., Nam, J.-M., Kojima, C., Mochizuki, N. and Sabe, H. (2009). EphA2 engages Git1 to suppress Arf6 activity modulating epithelial cell-cell contacts. *Mol. Biol. Cell* **20**, 1949-1959.

Monteiro, A. C., Sumagin, R., Rankin, C. R., Leoni, G., Mina, M. J., Reiter, D. M., Stehle, T., Dermody, T. S., Schaefer, S. A., Hall, R. A. et al. (2013). JAM-A

associates with ZO-2, afadin, and PDZ-GEF1 to activate Rap2c and regulate epithelial barrier function. *Mol. Biol. Cell* **24**, 2849-2860.

Morita, K., Itoh, M., Saitou, M., Ando-Akatsuka, Y., Furuse, M., Yoneda, K., Imamura, S., Fujimoto, K. and Tsukita, S. (1998). Subcellular distribution of tight junction-associated proteins (occludin, ZO-1, ZO-2) in rodent skin. *J. Invest. Dermatol.* **110**, 862-866.

Niessen, C. M. (2007). Tight junctions/adherens junctions: basic structure and function. *J. Invest. Dermatol.* **127**, 2525-2532.

Ooshio, T., Kobayashi, R., Ikeda, W., Miyata, M., Fukumoto, Y., Matsuzawa, N., Ogita, H. and Takai, Y. (2010). Involvement of the interaction of afadin with ZO-1 in the formation of tight junctions in Madin-Darby canine kidney cells. *J. Biol. Chem.* **285**, 5003-5012.

Orchard, S., Ammari, M., Aranda, B., Breuza, L., Briganti, L., Broackes-Carter, F., Campbell, N. H., Chavali, G., Chen, C., Del-Toro, N. et al. (2014). The MIntAct project—IntAct as a common curation platform for 11 molecular interaction databases. *Nucleic Acids Res.* **42**, D358-D363.

Pal-Ghosh, S., Tadvalkar, G., Jurjus, R. A., Zieske, J. D. and Stepp, M. A. (2008). BALB/c and C57BL6 mouse strains vary in their ability to heal corneal epithelial debridement wounds. *Exp. Eye Res.* **87**, 478-486.

Perez White, B. E. and Getsios, S. (2014). Eph receptor and ephrin function in breast, gut, and skin epithelia. *Cell Adh. Migr.* **8**, 327-338.

Roux, K. J., Kim, D. I., Raida, M. and Burke, B. (2012). A promiscuous biotin ligase fusion protein identifies proximal and interacting proteins in mammalian cells. *J. Cell Biol.* **196**, 801-810.

Roux, K. J., Kim, D. I. and Burke, B. (2013). BioID: a screen for protein-protein interactions. *Curr. Protoc. Protein Sci.* **74**, 19.23.1-19.23.14.

Schindelin, J., Arganda-Carreras, I., Frise, E., Kaynig, V., Longair, M., Pietzsch, T., Preibisch, S., Rueden, C., Saalfeld, S., Schmid, B. et al. (2012). Fiji: an open-source platform for biological-image analysis. *Nat. Methods* **9**, 676-682.

Schlessinger, J. (2014). Receptor tyrosine kinases: legacy of the first two decades. *Cold Spring Harb. Perspect. Biol.* **6**, pii:a008912.

Schneider, C. A., Rasband, W. S. and Eliceiri, K. W. (2012). NIH Image to ImageJ: 25 years of image analysis. *Nat. Methods* **9**, 671-675.

Searle, B. C. (2010). Scaffold: a bioinformatic tool for validating MS/MS-based proteomic studies. *Proteomics* **10**, 1265-1269.

Severson, E. A., Lee, W. Y., Capaldo, C. T., Nusrat, A. and Parkos, C. A. (2009). Junctional adhesion molecule A interacts with Afadin and PDZ-GEF2 to activate Rap1A, regulate beta1 integrin levels, and enhance cell migration. *Mol. Biol. Cell* **20**, 1916-1925.

Simpson, C. L., Kojima, S.-i. and Getsios, S. (2010). RNA interference in keratinocytes and an organotypic model of human epidermis. *Methods Mol. Biol.* **585**, 127-146.

Tanaka, M., Kamata, R. and Sakai, R. (2005). EphA2 phosphorylates the cytoplasmic tail of Claudin-4 and mediates paracellular permeability. *J. Biol. Chem.* **280**, 42375-42382.

Van Itallie, C. M., Tietgens, A. J., Aponte, A., Fredriksson, K., Fanning, A. S., Gucek, M. and Anderson, J. M. (2014). Biotin ligase tagging identifies proteins proximal to E-cadherin, including lipoma preferred partner, a regulator of epithelial cell–cell and cell–substrate adhesion. *J. Cell Sci.* **127**, 885-895.

Walsh, R. and Blumenberg, M. (2011). Specific and shared targets of ephrin A signaling in epidermal keratinocytes. *J. Biol. Chem.* **286**, 9419-9428.

Yamamoto, T., Harada, N., Kano, K., Taya, S., Canaani, E., Matsuura, Y., Mizoguchi, A., Ide, C. and Kaibuchi, K. (1997). The Ras target AF-6 interacts with ZO-1 and serves as a peripheral component of tight junctions in epithelial cells. *J. Cell Biol.* **139**, 785-795.

Zantek, N. D., Azimi, M., Fedor-Chaiken, M., Wang, B., Brackenbury, R. and Kinch, M. S. (1999). E-cadherin regulates the function of the EphA2 receptor tyrosine kinase. *Cell Growth Differ.* **10**, 629-638.

Zhou, N., Zhao, W.-D., Liu, D.-X., Liang, Y., Fang, W.-G., Li, B. and Chen, Y.-H. (2011). Inactivation of EphA2 promotes tight junction formation and impairs angiogenesis in brain endothelial cells. *Microvasc. Res.* **82**, 113-121.